Thermo-mechanical, morphological and water absorption properties of thermoplastic starch/cellulose foam composites reinforced with PLA

Mohammad M. Hassan*[a,d], Marie J. Le Guen [b,d], Nick Tucker [c,d,†], Kate Parker [b,d]

[a] Food & Bio-based Products Group, AgResearch Limited, Private Bag 4749, Christchurch 8140, New Zealand.

[b] Scion, 49 Sala Street, Rotorua 3010, New Zealand.

[c] University of Lincoln, School of Engineering, Brayford Pool, Lincoln, LN6 7TS, United Kingdom.

[d] Biopolymer Network (BPN), 49 Sala street, Rotorua 3010, New Zealand.

***Correspondence to:**

Mohammad Mahbubul Hassan

Food & Bio-based Products Group, AgResearch Limited, Private Bag 4749, Christchurch 8140, New Zealand.

E-mail: mahbubul.hassan@agresearch.co.nz

[†] Present address: School of Engineering, University of Lincoln, Brayford Pool, Lincoln LN6 7TS, U.K.

Abstract

Expanded polystyrene foams are lightweight, cheap, and have excellent strength and insulation properties however their inability to biodegrade in traditional landfill sites made their disposal problematic. Starch, a polysaccharide, has the potential to replace synthetic thermoplastics for some applications but starch-based foams are hydrophilic, which limits their applications. In this work, polylactide (PLA), a sustainably derived and industrially compostable polymer was added to starch/cellulose composite foams to enhance their water barrier properties. PLA powder at various weight% was mixed with moistened starch and cellulose mixture and composite foams were prepared by compression moulding at 220 °C. The thermomechanical and viscoelastic properties of the produced foam materials were analysed by thermogravimetric analysis, dynamic mechanical thermal analysis and also by the 3-point compressive mechanical quasi-static testing. It was found that flexural strength increased and the water absorption properties decreased with an increase in PLA weight (%) in the starch/cellulose foam composites.

Key words Biocomposite foams . Starch/cellulose composites . PLA . Rheology . Thermomechanical properties

Introduction

Depletion of petrochemical resources, together with the accumulation of non-biodegradable plastics in the environment have led to renewed interest in the development of packaging from biomasses and other sustainable resources. Traditionally, cellulose and thermoplastic

polymers have been used in the manufacturing of packaging. However, sustainable cellulose-based packaging materials (paper and cardboard) have limitations, particularly due to their poor water barrier properties that restrict their use in many applications. In addition, when they encounter water, they slowly lose their strength and finally disintegrate. Most of the popular thermoplastic polymers currently used in packagings, such as low-density polyethylene (LDPE) and polypropylene (PP), are not biodegradable or of sustainable origin. Only a small percentage of plastic packaging is collected for recycling and therefore most of it is still ending up in a landfill, effectively polluting our environment. Biodegradable plastics can address this problem and are therefore increasingly replacing non-biodegradable and petrochemical-derived commodity plastics in packaging applications. The most promising synthetic biodegradable plastic is polylactic acid (PLA), which is made from corn by converting corn starches to sugar, which is then converted to lactic acid (the monomer of PLA) through various fermentation stages (Rahman et al. 2011).

Starch is abundant and cheap, and can be sourced from a number of convenient crops such as potato, rice, wheat, corn, tapioca, cassava, often as a co-product, so not reducing the amount of starch availble as a foodstuff. In the presence of a plasticiser, at high temperatures and pressures, starch loses its crystallinity and becomes thermoplastic allowing processing using traditional thermoplastic processing machinery, such as injection moulding (Swanson et al. 1993; Stepto 2006; Soukeabkaew et al., 2015). Although thermoplastic starch is biodegradable, the poor mechanical strength limits its application (Dos Santos et al. 2018). A range of fibrous materials and clays including β-carotene (Kim and Huber 2016), nanoclay (Romero-Bastida et al. 2016), kaolinite (Mbey and Thomas 2015), sugarcane bagasse fibres (Dos Santos et al. 2018), flax fibres (Romero-Bastida et al. 2016), date palm fibres (Ibrahim et al. 2017), jute fibres (Wang et al. 2017; Soykeabkaew et al., 2015; Soykeabkaew et al., 2004), cellulose nanocrystals (Ali et al. 2018; Tabassi et al. 2016), β-glucan (Sagnelli et al.

66 2017), wheat gluten (Muneer et al. 2015), sugar palm fibres (Edhirej et al. 2017), and
67 cellulose nanowhiskers (Liu et al. 2017), has been investigated to enhance its mechanical
68 properties. Blending with various natural and synthetic polymers, such as zein (Corradini et
69 al. 2006), chitosan (Mendes et al. 2016), natural rubber (Carmona et al. 2014), and the
70 aliphatic polyester (Martin et al. 2001) has been investigated for the same purpose.

71 Foam packaging is very popular because it is low density and has good thermal insulation
72 properties. For example, non-biodegradable expanded polystyrene (EPS)-based foam
73 packaging is extensively used for low0cots hot and cold food packaging. Thermoplastic
74 starch-based foams have also been investigated for packaging applications as they have
75 thermal insulation properties comparable with currently used EPS foams (Deng and
76 Catchmark 2014; Zhou et al. 2006). Starch-made materials have thermal insulation properties
77 comparable with commercial competitors (Glenn et al., 2001a). However, starch foams
78 respond poorly to high moisture conditions because of their high hydrophilicity (Glenn et al.
79 2001b). At high humidity or in contact with water they lose strength, shape and structural
80 integrity (Shogren et al. 1998). Conversely, at low humidity conditions, they lose their plastic
81 properties and become brittle. It was found that the increase in amylose content in the starch
82 produces denser and stronger foams with a sacrifice in flexibility (Noorbakhsh-Soltani et al.,
83 2018). Starch with a high amylopectin content produces light-weight foams but with poor
84 strength (Lawton et al., 1999). The addition of microfibrillated cellulose to starch also has
85 been extensively investigated to make the starch-made materials strong (Kaushik et al. 2010;
86 Hietala et al. 2013; Spiridon et al. 2014). The application of various plasticisers including
87 glycerol has been demonstrated to decrease the brittleness of starch-based materials (Avérous
88 et al. 2000; Ghanbari et al. 2018). Sometimes, starch-based articles are coated with a
89 thermoplastic polymer to improve their water barrier properties. However, if holes are formed
90 on the surface of the thermoplastic coating, their water barrier properties are compromised.

Natural rubber latex has been extensively investigated to improve the barrier properties of starch-based foams (Subramaniam 1990).

PLA is a hydrophobic polymer that fully degrades under certain conditions (Ghorpade et al. 2001). Masmoudi et al. reported the development of plasticised starch and cellulose reinforced PLA films (Masmoudi et al., 2016) and both types of films were fully biodegradable but the plasticised starch film showed quicker biodegradation compared to the other film.

Cellulose fibre, microfibrillated cellulose, cellulose nanocrystals, and PLA have been investigated as a reinforcing agent for the strengthening of starch-based films and foams [Patil et al., 2016; Shirai et al., 2013, Soykeabkaew et al., 2012]. The addition of PLA to tapioca starch in the presence of glycerol and other plasticisers, increased the tensile strength of starch/PLA foam to 1.31±0.06 MPa at 30% PLA loading and also the moisture content decreased [Preechawong et al., 2005]. The addition of cellulose enhanced the strength of starch-based films but the addition of PLA to starch enhanced the water barrier properties of the produced starch films. Starch/cellulose composite foam-based packaging has already been marketed by Earthpac (https://earthpac.co.nz), Paperfoam, and others, being marketed as an alternative to paper-based packaging, but their very poor water barrier properties make them unsuitable for the replacement of hydrophobic EPS foam packaging. To the best of our knowledge, no published literature reported the enhancement of the water barrier properties and flexural strength of starch/cellulose foam composites by the addition of PLA. It is known that PLA films have considerably higher moisture barrier properties compared to starch films [Muller et al., 2016]. Therefore, we envisaged that the addition of PLA to potato starch/cellulose composite foam not only would enhance its strength but also its moisture and oxygen gas barrier properties. However, it is quite difficult to make a uniform blend of PLA pellets with starch/cellulose powders, especially at ambient temperature. Therefore, we used

PLA powder to facilitate the uniform mixing of PLA with starch/cellulose powders for the production starch/cellulose/PLA foam composites. In this work, we are reporting a simple room temperature mixing and high-temperature short-time compression moulding method for the development of cheap but fully biodegradable starch/cellulose/PLA foam composite with considerably higher water barrier properties compared to the starch/cellulose foams that potentially can replace the currently used EPS packaging.

Table 1 The composition of starch/cellulose/PLA foam composites

Sample ID.	Dry weight (%)			
	Starch	Cellulose	PLA	Carnauba wax
Control	72.80	24.30	-	2.90
Composite 1	70.35	24.30	2.45	2.90
Composite 2	67.94	24.30	4.86	2.90
Composite 3	65.42	24.30	7.28	2.90
Composite 4	63.08	24.30	9.72	2.90

Experimental section

Materials

Potato starch and carnauba wax were procured from Earthpac Ltd, Auckland, NZ. The potato starch has an average granule size of 96 μm and approximately 16% moisture and is

132 composed of 28.6% amylose and 71.4% amylopectin. Cellulose fibre powder (500 to 800 µm
133 long and 15 to 34 µm wide) was purchased from FineCel Sweden AB (Stockholm, Sweden).
134 PLA powder was produced by cryogenic milling of PLA pellets (Ingeo 2003D, NatureWorks,
135 USA, molecular weight M_n = 114317 g/mol measured by GPC) and the particle size was
136 approx. 300 to 700 µm. The average size of the PLA powder was 500 µm.

137

138 Preparation of Starch/cellulose/PLA foam composites

139

140 Because of the difficulty of uniformly mixing of PLA pellets to starch/cellulose powders,
141 PLA was ground to powder by cryogenic milling. The weight (%) of cellulose fibre powder
142 and carnauba wax was kept fixed and the weight (%) of PLA and starch were varied.
143 Carnauba wax used as a plasticiser and internal mould release agent. A small quantity of
144 water (40 ml) was added to obtain the disruption of the native starch and to decrease the melt
145 viscosity during compression moulding. Thermoplastic starch matrix behaviour varies
146 depending on the formulations with a variation of glass transition temperature (Avérous et al.
147 2000). The processing stages begin with the dry blending of starch, cellulose fibre powder,
148 and carnauba wax. Table 1 shows the compositions of various composites. Starch, cellulose,
149 and carnauba wax were mixed together in the presence of a small amount of water and then
150 the mixture was compression moulded to prepare the foam composites. The composite
151 fabrication method is shown by a schematic diagram in Fig. 1. They were mixed together at
152 slow speed using a food mixer followed by the addition of water with continuous stirring to
153 obtain a uniform granular mixture. The final moistened mixture was obtained after an high
154 speed mixing at 1500 rpm for 60 s.

85 g aliquots of the mixture was compression moulded in a plate-shaped mould tool at 220 °C for 60 s to convert the mixture into foam composite plates. The starches were quickly gelatinised and dry foam plates were prepared by quick evaporation of water and volatiles during the compression moulding. To improve the water barrier properties of potato starch/cellulose plates, PLA powder was added to the potato starch/cellulose mixture at 2.45, 4.86, 7.28 and 9.72 %. The foam composite samples were then cut into various sizes to carry out various characterisations.

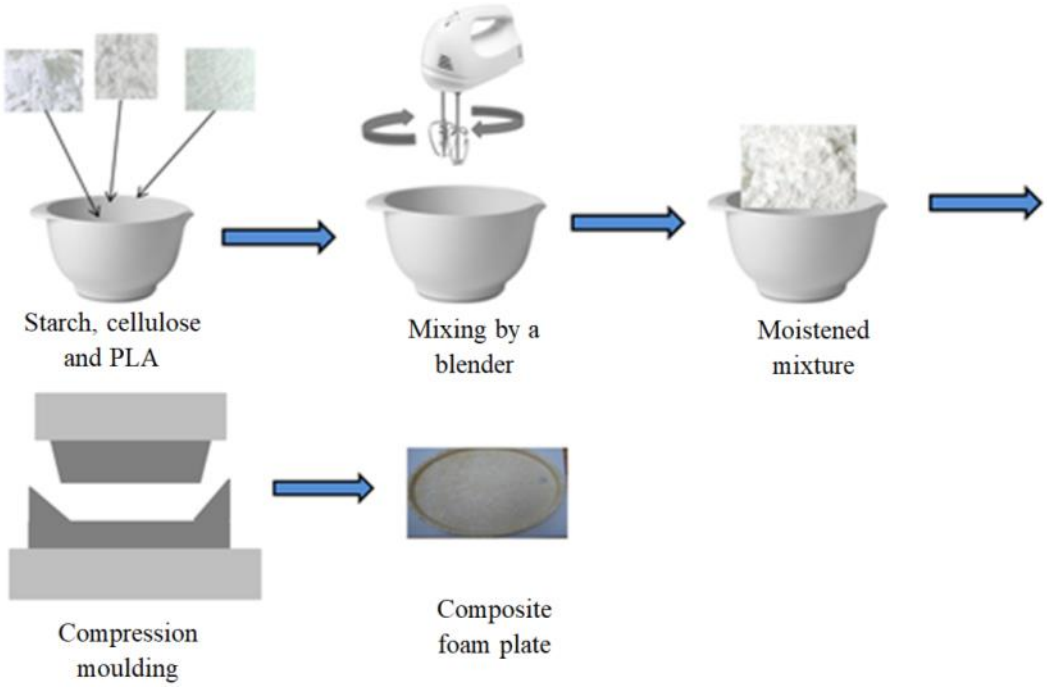

Fig. 1 The schematic diagram of the preparation of PLA-reinforced starch/cellulose composite foam.

Physicochemical and mechanical characterisations

169 The *CIE L*a*b** colour measurements of the starch/cellulose foam composites were carried
170 out with a Mahlo spectrophotometer (Color eye 40/0, Mahlo GmbH, Germany) under D65
171 illuminant and 10° observer and the whiteness index was calculated according to the
172 following equation:

173 $$Whiteness\ index = 100 - [(100 - L^*)^2 + (a^*)^2 + (b^*)^2]^{0.5} \quad (1)$$

174 Thermo-gravimetric analysis (TGA) was carried out in a TA Instruments' Discovery TGA
175 (Model 550, TA Instruments Inc., New Castle, USA) from room temperature to 500 °C at a
176 heating rate of 5 °C/min under nitrogen environment. 15 × 56 × 1.5 mm size samples with
177 various PLA loadings were cut and dynamic mechanical thermal analysis (DMTA) was
178 carried out in a 3-point static flexural mode using a dynamic mechanical analyser (Model
179 RSA-G2, TA Instruments, New Castle, USA). The measurements were dynamic time sweep
180 tests starting from T = 25 °C to 80 °C at a heating rate of 5 °C/min and frequency fixed at 1
181 Hz. The storage modulus (E'), loss modulus (E''), and loss factor (tan δ) of the samples were
182 measured.

183 The flexural strength was measured by a 3-point flexural test rig attached to an Instron
184 Universal Tensile Testing machine at a crosshead speed of 2 mm/min at the standard
185 atmospheric conditions (20±2 °C and 65±2% relative humidity) using a span length of 34.5
186 mm. The sample size was 60 × 15 × 1.5 mm and samples were pre-conditioned for 48 h. The
187 vertical displacement was measured at the centre of the disc using an LVDT displacement
188 transducer. The samples were preconditioned for 48 h before measuring. For each sample, at
189 least 10 tests were carried out and the averages are reported here.

190 The contact angle was measured in dynamic mode by using a KSV CAM 100 Contact
191 Angle Measurement Apparatus (KSV Instruments, Helsinki, Finland) and the Young-Laplace
192 equation was used to quantify the contact angles. For each sample, the contact angle was

measured at 5 places and the average contact angle was reported. The first measurement was taken immediately after placing the drop of water and then at 120 s interval measurements were taken until 480 s. The ordinary and the cracked surface of composite foams were characterised by scanning the surface without any conductive coating in the backscattered mode on a Hitachi scanning electron microscope or SEM (Model: TM3030Plus, Hitachi Corporation, Japan) at an accelerating voltage of 15 kV.

The water absorption by a control starch/cellulose composite and also the composites containing various weight (%) of PLA was measured according to *ASTM Test Method D570: Standard Test Method for Water Absorption of Plastics*. 4 cm × 4 cm × 0.2 cm size samples were immersed in distilled water at room temperature after which they were removed from the tank after 10, 20, 30, 60, and 240 min, water adhered on the surface was wiped by a tissue paper and weighed. Finally, the water uptake was calculated as the mass difference and expressed as a percentage. The IR spectra of the composite foam surfaces were recorded using a PerkinElmer FTIR (Model: System 2000, PerkinElmer Corporation, USA) with an attenuated total reflectance (ATR) attachment using a Zn/Se ATR crystal. The fabric samples were placed flat on the upper side of the crystal. Good fibre to crystal contact was ensured by applying 50 N force using a calibrated torque wrench. 64 scans were carried out for each sample and the averages are reported here.

Results and discussion

Physical characteristics and colour

Fig. 2 shows the visual appearance of control starch/cellulose foam composite and also starch/cellulose foam composites containing various weight (%) of PLA. It can be seen that the surface of the composites are quite smooth with no visible pores. The colour of the composites changed from yellowish with no PLA, to brownish with various weight (%) of PLA. The increase in PLA loading had a marginal effect in changing the colour of the starch/cellulose foam composites.

Table 2 shows the *CIE L*a*b** values and whiteness index of starch/cellulose foam composites containing various weight (%) of PLA. The colour of the foam composite started to become lighter and reddish with the addition of PLA as the value of *L** increased by the addition of PLA. The lightness value (*L**) of the control starch/cellulose foam composite was

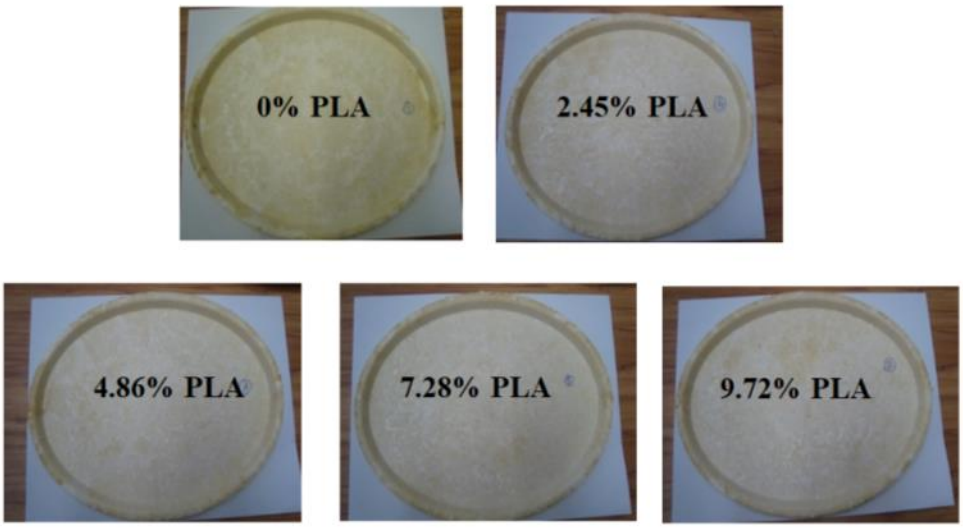

Fig. 2 Visual appearance of starch/cellulose composite foam plates containing various weight (%) of PLA.

93.54, which increased to 95.71 for the starch/cellulose composite foam containing 2.45% PLA. Further increase in the PLA loading had little effect on the value of as its value only

slightly reduced. The addition of PLA initially increased the redness and decreased the yellowness of the composite. However, the redness (a^*) decreased and yellowness (b^*) increased with an increase in the PLA loading. The control sample was more yellowish compared to the starch/cellulose foam composites with various PLA loadings. The addition of PLA to starch/cellulose foam composite increased its redness (a^*) but decreased the yellowness (b^*) up to 2.45% PLA loading but further increase in the PLA loading slightly decreased redness but increased the yellowness. It is evident that the addition of PLA had a marginal effect on the whiteness index of starch/cellulose foam composites as the whiteness index increased from 84.6 to 85.9 for the 0 to 2.45% PLA but the whiteness index decreased to 85.1 with an increase in the PLA loading.

Table 2 Colour and whiteness index of PLA-reinforced potato starch/cellulose foam composites containing various PLA loadings.

PLA loading (%)	*CIE*			Whiteness index
	L*	a*	b*	
0	93.54	1.15	13.97	84.6
2.45	95.71	1.98	13.29	85.9
4.86	95.56	1.90	13.65	85.5
7.28	95.37	1.88	13.84	85.3
9.72	95.02	1.82	13.89	85.1

Thermo-gravimetric analysis (TGA)

TGA was carried out to observe whether the addition of PLA has any effect on its thermal stability of the composite foams. As expected the weight loss of all starch/cellulose/PLA composite foams increased with an increase in the temperature due to the formation of volatiles by the decomposition of the cellulose, starch, and PLA as shown in Fig. 3. Of the samples, neat PLA showed the best thermal stability but showed the lowest char yield. On the other hand, the starch/cellulose foam composite without any PLA showed the worst thermal stability. The addition of PLA to starch/cellulose foam composites improved the thermal stability of the composite foams, which improved with an increase in the weight (%) of PLA in the composite foams. It can be seen that for all samples the weight loss occurred at five stages, 60 – 120 °C, 120 – 278 °C, 278 – 327 °C, 327 – 362 °C, and 362 – 600 °C, except neat PLA for which the weight loss occurred at three stages, 60 – 305 °C, 305 – 380 °C, and 380 – 600 °C. For all composite samples, from room temperature to 320 °C a small weight loss was observed. but for neat PLA almost no weight loss was observed up to 277 °C as PLA absorbs no moisture: starch and cellulose both absorb moisture. The weight loss occurring in the composite samples in the 60 to 120 °C region is likely due to the loss of absorbed moisture (Orue et al. 2016), which decreased with an increase in the PLA loading. At 120 – 277 °C, the least weight loss was observed for all composite samples and less than 3% weight was lost at this stage.

Fig. 3 (bottom) shows the DTG curves of neat starch/cellulose foam composite material and also composites with various PLA loadings. For all composite foams, the maximum degradation occurred in the temperature range of 278 to 327 °C, where approximately 65% weight loss was observed. For the control starch/cellulose foam composite the maximum degradation occurred at 315.65 °C, which increased to 316.4, 116.9, 319.5 and 320 °C for the starch/cellulose composites with 2.45, 4.86, 7.28 and 9.72% PLA loadings. The second highest degradation of the control composite occurred at 349 °C, which increased to 349.6,

351.7, 356.3 and 357.1 °C for the PLA loading 2.45, 4.86, 7.28 and 9.72% respectively. On the other hand, the maximum degradation of PLA occurred at 363 °C. The rapid weight loss was observed in this stage due to depolymerisation and degradation of cellulose, starch, and PLA producing volatile compounds including carbon dioxide and carbon monoxide. The highest weight loss was observed for the neat PLA as the weight loss increased from 0.6% to 97.2% at 375 °C.

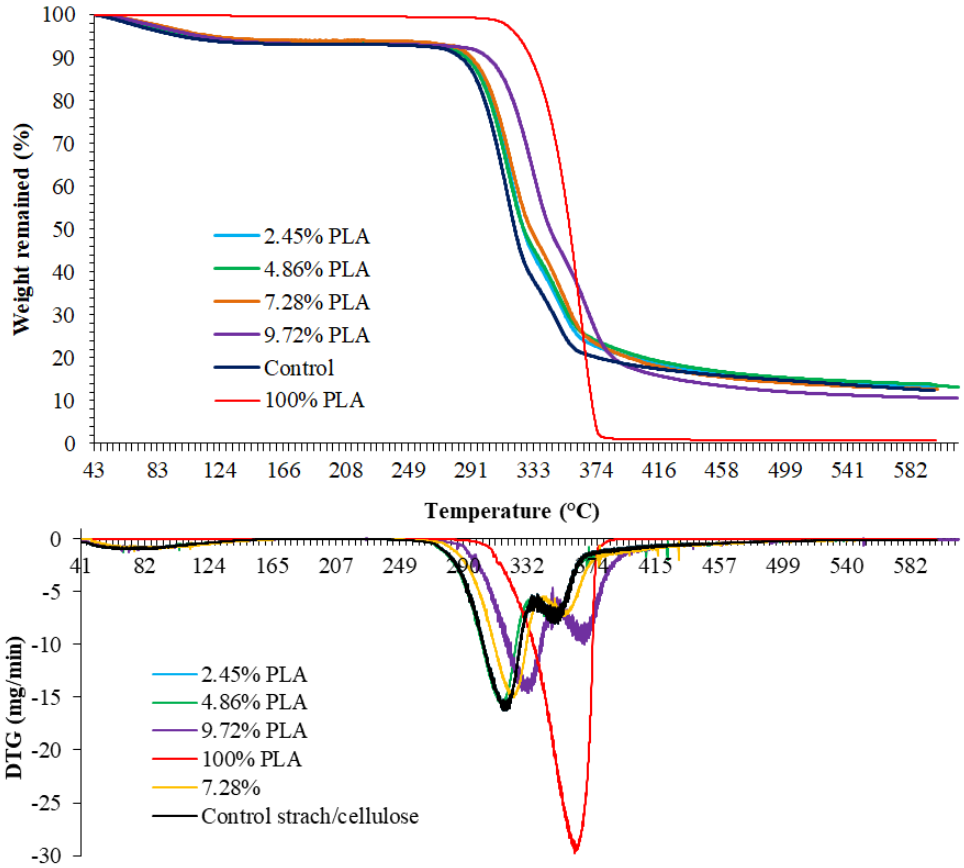

Fig. 3 Thermo-gravimetric (top) and DTG (bottom) curves of potato starch/cellulose/PLA foam composites with various weight of PLA.

Dynamic mechanical thermal analysis (DMTA)

DMTA was carried out to determine the effect of the addition of PLA to the starch/cellulose foam composites had on their storage modulus (*E'*) and loss modulus (*E''*) at various temperatures, and also to understand their viscoelastic behaviour. Fig. 4 represents the storage modulus (*E'*) and loss modulus (*E''*) curves of starch/cellulose composite foams containing various weight % of PLA from room temperature to 200 °C. It is evident that for all the composite samples the storage modulus decreased with an increase in the temperature due to the loss of stiffness of the composite materials.

The control and the starch/cellulose sample containing 2.45% PLA had the highest stiffness at all temperatures. The composite containing 2.5% PLA showed marginally higher storage modulus up to 58 °C, but beyond that temperature, the control starch/cellulose composite showed higher storage modulus up the maximum tested temperature. We have to remember that the glass transition temperature of PLA is 58 °C, i.e. below 58 °C it shows glassy nature and after 58 °C, it shows the characteristics of rubber. Therefore, up to 58 °C, the addition of PLA had a small effect on the stiffness of the starch/cellulose composite but above 58 °C the addition of PLA had a greater effect on the stiffness of the composite. At 30 °C, the storage modulus of the control starch/cellulose composite foam was 8.12×10^2 MPa, which increased to 8.53×10^2 MPa and then decreased to 7.89×10^2, 7.80×10^2 and 7.69×10^2 MPa for the cellulose/starch composite foam containing 2.45, 4.86, 7.28 and 9.72% PLA respectively. Compared to this, the control sample showed a storage modulus of 6.18×10^2 and 5.19×10^2 MPa 86 and 170 °C respectively. The corresponding values for the PLA with 2.45, 4.86, 7.28 and 9.72% PLA loadings were 6.03×10^2 and 5.00×10^2, 5.56×10^2 and 4.50×10^2, 5.09×10^2 and 4.06×10^2, and 3.56×10^2 MPa respectively. Overall, the storage modulus of starch/cellulose composites decreased with an increase in the PLA loading. The starch/cellulose composite with a higher loading of PLA (9.72 weight %) showed considerably higher stiffness at all temperatures. The loss modulus accounts for the viscous

component of the complex modulus or the out of phase component with the applied strain. The loss modulus also increased with an increase in the weight % of PLA in the starch/cellulose composites. It can be concluded that the addition of PLA to starch/cellulose composites had a negative effect on their stiffness.

The loss factor, Tan δ, is the ratio between the storage modulus and loss modulus, which represents mechanical damping or internal friction in a viscoelastic system. A high Tan δ value indicates that the material is inelastic and a low value indicates that the material is elastic.

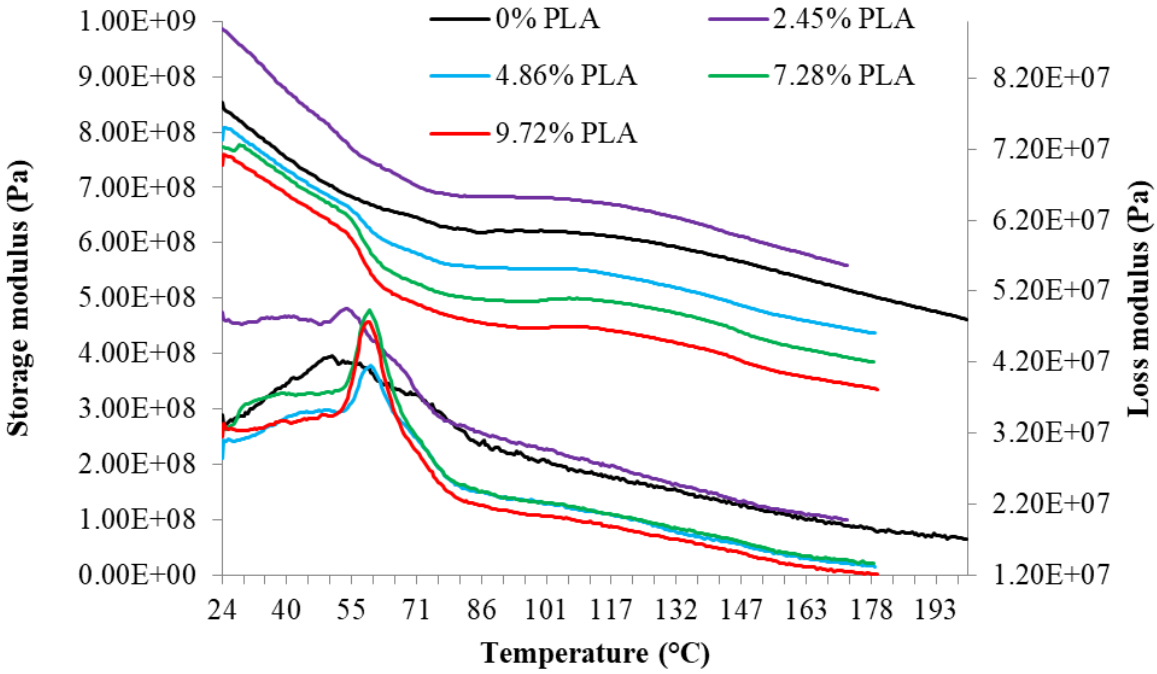

Fig. 4 Storage modulus and loss modulus of starch/cellulose composites containing various weight (%) of PLA at various temperatures.

The effect of adding PLA to the composites is expressed as a mechanical loss factor, Tan δ, as a function of temperature (Fig. 5). The Tan δ curve peak, which is indicative of the glass transition temperature (T_g), is also indicative of the degree of crosslinking of the system. The

control starch/cellulose composite does not show a sharp Tan δ peak, commonly associated with the T_g of a material, rather shows a very broad peak, i.e. does not show any defined transition temperature. The starch/cellulose composites containing PLA had sharp Tan δ peaks. The starch/cellulose composite material containing 2.45% PLA shows a glass transition temperature of 58 °C, which increased to 60.8, 60.75 and 61.3 °C for the 4.86, 7.28 and 9.72% PLA, respectively.

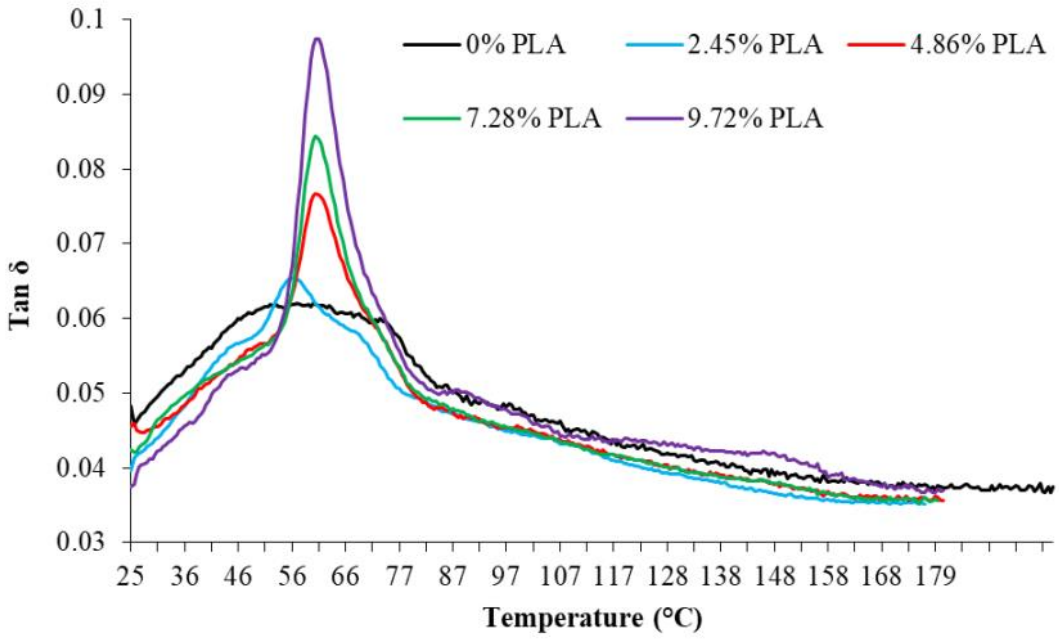

Fig. 5 The effect of the addition of PLA to the Tan δ of starch/cellulose composites as a function of temperature.

The composite containing 2.45% shows glass transition temperature at 56 °but further PLA loading increased the T_g to 58 °C presumably because of the presence of PLA. The increase in peak height of Tan δ with an increase in the loading of PLA suggests that the rigidity of the starch/cellulose composite foam increased with PLA level. The observed results are consistent with the results achieved by others (Avérous et al. 2001).

344

345 Effect of PLA loading on the flexural properties of composites

346

347 The 3-point bending flexural test was carried out to observe whether the addition of PLA
348 improves the rigidity/stiffness of the composite foam. The 3-point flexural test is a simple
349 way to subject a specimen to tension, compression, and shear simultaneously. The effect of
350 PLA loading on the flexural or bending strength of starch/cellulose is presented in Fig. 6
351 (top). It can be seen that the addition of PLA to starch/cellulose blends had a positive effect
352 on the flexural strength of the produced foams composites. The lowest flexural strength was
353 observed for the control starch/cellulose and the highest for the starch/cellulose foam
354 composite containing 9.72 % PLA. The flexural strength of the starch/cellulose composites
355 increased with an increase in the weight (%) of PLA. The strength of the starch/cellulose
356 composite foam was increased from 4.33 MPa for the control to 4.867 MPa for the
357 starch/cellulose composite with 9.72% PLA, a 14.8% increase in the bending rigidity. The
358 increase in the flexural strength indicates improved adhesion between matrix starch and PLA,
359 and also between cellulose and PLA. Therefore, it can be concluded that the addition of PLA
360 to the starch/cellulose composite had a reinforcing effect in increasing their flexural strength.

361 It was reported that the tapioca starch/PLA composites containing 0% PLA exhibited flexural
362 strength of approximately 1.0 MPa at 65% relative humidity [Preechawong et al., 2005], but
363 in our case, the flexural strength increased to 4.97 MPa due to the reinforcing effect of
364 cellulose fibre.

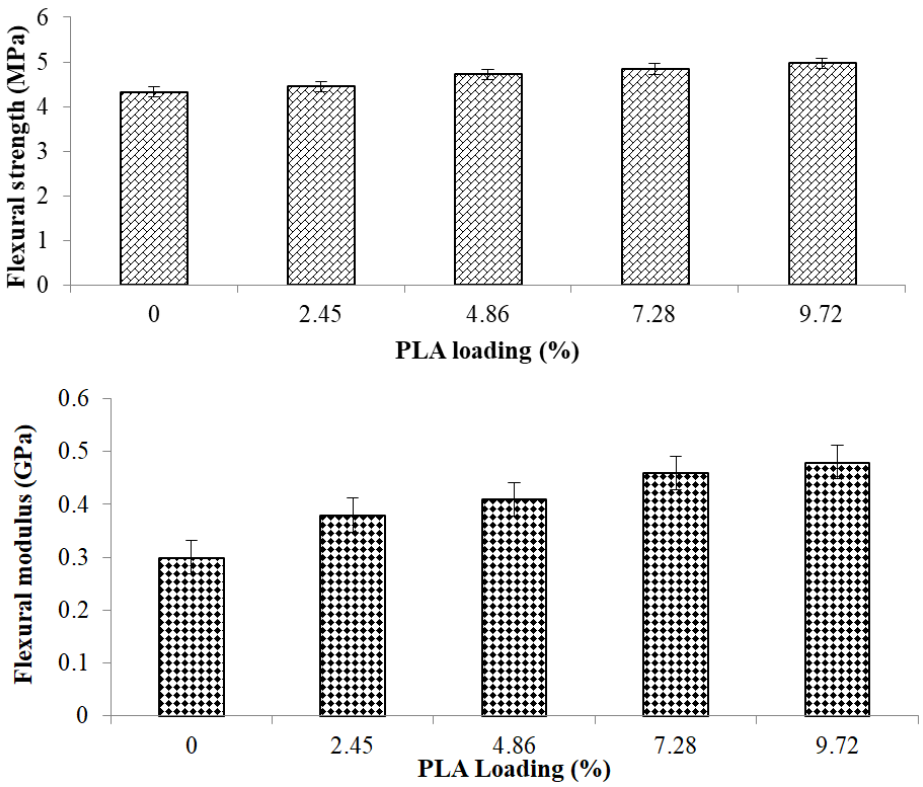

Fig. 6 Effect of addition of PLA on the flexural strength (top) and flexural modulus (bottom) of starch/cellulose composites.

Fig. 6 (bottom) shows the effect of PLA loading on the flexural modulus of the starch/cellulose foam composites. Like flexural strength, the flexural modulus also increased with an increase in the PLA loading. The lowest flexural modulus was exhibited by the control starch/cellulose composite and it was 0.3 GPa, which increased to 0.48 GPa for the PLA loading of 9.72%. The flexural modulus of starch/cellulose composite almost 50% increased for the 9.72% PLA loading.

Cross-sectional and surface morphologies

Composites fracture surfaces were examined using scanning electron microscopy (SEM) to observe the effect of the addition of PLA on the microstructure (Fig. 7). The skin layer of all composites exhibited small, dense, and closed cell foam structure. However, the interior of the foam composites show quite large and opened cell structure. The size and distribution of the cells over the region are non-uniform. The dense outer skin layer was formed due to the abruption of evaporation of water molecules in the PLA-rich batter layer adjacent to the hot surface of mould [Preechawong et al., 2005]. The control starch/cellulose foam composite shows larger cells compared to the composites containing various weight (%) of PLA. In the interior of the foam composites, large opened cells were formed due to the boiling of a large amount of water, which expanded the pores before collapsing the pore walls during high-temperature moulding [Lawton et al., 1999]. The control starch/cellulose composite showed quite different morphologies compared to the starch/cellulose composites containing various weights (%) of PLA. The starch/cellulose composites containing 4.86 and 7.28% of PLA showed relatively uniform distribution of cells and uniform size of cells compared but smaller cells than the control starch/cellulose composite. Starch/cellulose composite containing 9.72% of PLA showed some smaller cells but also some large cells, larger than the one observed for the control starch/cellulose foam composite. It is also evident that inside the starch/cellulose foam composites all starch granules were gelatinised as no starch granules are visible.

The SEM images of the surfaces of the starch/cellulose composite foams with increased loading of PLA are shown in Fig. S1 (Supplementary Material). For the control sample, the cellulose fibre is visible on the surface. It is evident that some of the starch granules were not fully gelatinised during processing and did not expand but bonded to the rest of the fully gelatinised starch. The surface of the foam composites became smoother with increased loading of PLA, especially for 7.28 and 9.72% of PLA loading. PLA spread and covered the

surface of foam composites as the moulding temperature used was considerably high and looks like fully melted during the short moulding time. It is evident that PLA shows quite good adhesion with gelatinised starch, which likely contributes to the increased stiffness observed by mechanical testing.

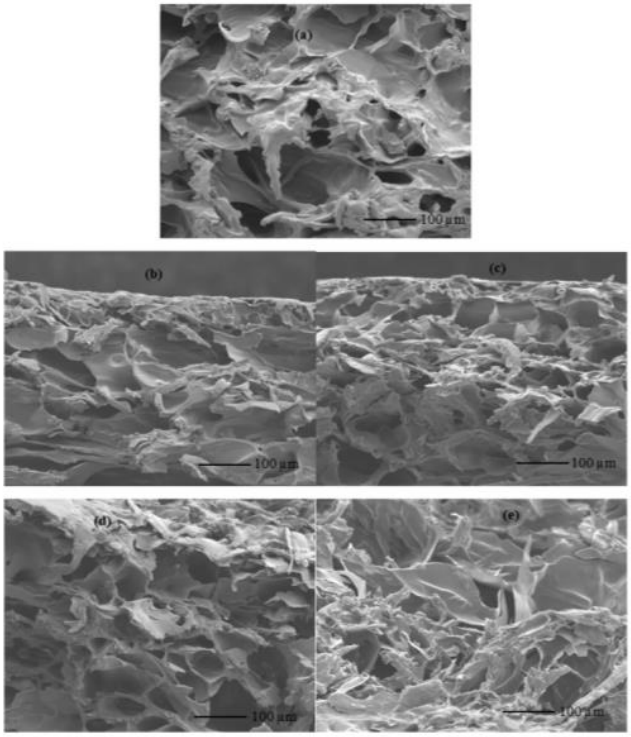

Fig. 7 SEM images of control starch/cellulose composite (a) and also starch/cellulose composites with 2.45 (b), 4.86 (c), 7.28 (d) and 9.72% (e) of PLA.

Dynamic contact angle

The water contact angle of composite foam was measured to determine whether the addition of PLA to the composites increases their surface hydrophobicity and water barrier properties. Fig. 8 shows the optical image of contact angle and water droplet shape at different times of surface of starch/cellulose foam composites having different PLA loading. From the dynamic

417 water contact angle data of the surface of various composites, it is evident that the addition of
418 PLA to starch/cellulose composites increased hydrophobicity (Table S1 in Supplementary
419 Material). It is expected that the surface of the control starch/cellulose composite would be
420 hydrophilic as both starch and cellulose are strongly hydrophilic but it showed very low
421 hydrophilicity. The control composite in these tests contains wax that probably increased the
422 hydrophobicity, which is evident in the high contact angle shown for the control.

423 For the control starch/cellulose foam, the contact angle at 0 s was 102.3° that decreased to
424 only 95.4° after 480 s showing some levels of hydrophobicity. The strong hydrogen bonding
425 between hydroxyl groups of starch and cellulose along with carnauba wax might have
426 contributed to increasing the hydrophobicity of the control starch/cellulose composite. On the
427 other hand, the contact angle of the composites increased with an increase in the PLA loading
428 and the contact angle was quite stable over 480 s indicating their excellent hydrophobicity.
429 The composite foam with 9.72% PLA loading showed the highest contact angle and it was
430 120.7°. The control starch/cellulose foam composite showed the lowest hydrophobicity as the
431 contact angle decreased with time. The starch/cellulose composite containing 9.72% showed
432 the highest contact angle and it was stable until the end of the test. The results indicate that
433 the addition of PLA improved hydrophobicity or water barrier properties of the composites.

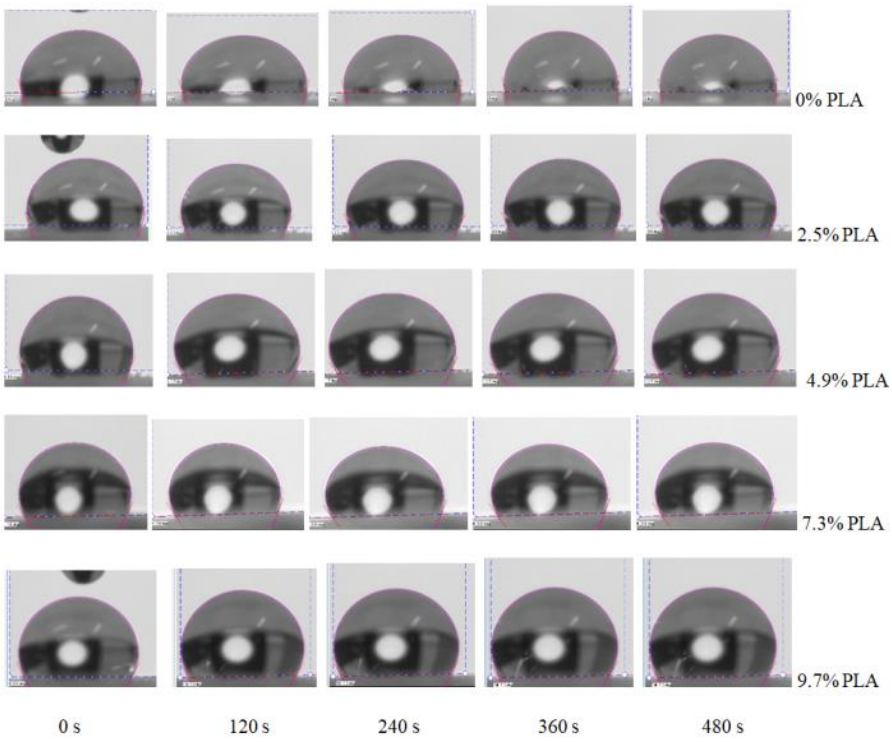

434

435 **Fig. 8** Optical images of changing contact angle at a different time for the surface of
436 starch/cellulose composites containing various PLA loadings.

437

438 Water absorption

439

440 Water resistance of these samples was further investigated by carrying out a water absorption
441 test. As expected, the control composite foam without PLA showed the highest absorption of
442 water (Fig. S2 in Supplementary Material). The water absorption rate was highest in the first
443 10 min, after which the water absorption rate slowed but still showed an increase over time.
444 All the other composites showed similar behaviour.

445 The composites containing 2.45, 4.86 and 7.28% PLA showed very similar water
446 absorption but with an increase in time, considerable differences in water absorption were
447 observed for the various weights (%) of PLA. The water absorption performance of

448 starch/cellulose composites decreased with an increase in the weight (%) of PLA and the
449 composite containing 9.72% PLA showed the lowest water absorption. The starch/cellulose
450 composites containing 2.45, 4.86 and 7.28% PLA showed similar levels of water absorption
451 but the composite containing 9.72% PLA showed considerably lower water absorption
452 compared to the control starch/cellulose and other PLA containing composites. It can be
453 concluded that the addition of PLA to the starch/cellulose composite had a positive effect in
454 increasing their water barrier properties.

455

456 Attenuated Total Reflectance Fourier-transform infrared spectroscopy (ATR-FTIR)

457

458 The ATR-FTIR spectra of starch/cellulose composites containing PLA loadings are shown in
459 Fig. S3 (Supplementary Material). The spectrum of control starch/cellulose composites shows
460 characteristics bands of starch and cellulose at 758, 847, 930, 992, 1014, 1078, 1150, 1249,
461 2849, 2917, and broadband at 3255 cm^{-1}. The spectrum of control starch/cellulose composites
462 shows four characteristic bands between 980 and 1160 cm^{-1} (992, 1014, 1078 and 1150 cm^{-1})
463 corresponding to the C−O bond stretching band attributed to primary alcohols (Marechal and
464 Chanzy, 2000). The band at 1150 cm^{-1} can be assigned to the C−O−C asymmetric stretching
465 vibrations, which shows that ether bonds were formed between the primary alcohol groups of
466 starch resulting in a decrease in hydrophilicity. There is a new ester band formed at
467 1178 cm^{-1}, which came from the ester groups of PLA for the spectra of composites with PLA
468 loading 4.86% and more, indicating the presence of PLA at the surface of the composite
469 foams. The bands at 1315 and 1430 cm^{-1} can be assigned to CH_2 wagging symmetric bending
470 and CH_2 asymmetric bending, respectively (Kacurakova et al. 2002). The absorption band at
471 1648 cm^{-1} is due to an intermolecular hydrogen bond involving the carboxyl groups. The
472 bands at 2849 and 2917 cm^{-1} are due to symmetric and asymmetric C-H stretching vibrations.

The broadband at 3255 cm^{-1} can be attributed to hydroxyl groups of starch and cellulose. The spectra of starch/cellulose composites containing various PLA loadings (%) show similar peaks but it is evident that the intensity of the broad hydroxyl peak at 3225 cm^{-1} decreased with an increase in the weight (%) of PLA. The reduction in the intensity of OH band indicates that the foam composite became more hydrophobic with an increase in the PLA loading in the composite foams.

Conclusions

We have demonstrated that the incorporation of PLA to starch/cellulose matrix modified the physical and chemical properties of starch-based composite materials bringing considerable improvements in water barrier properties, stiffness, and flexural strength. The addition of PLA to starch/cellulose composites slightly improved their thermal stability by increasing the peak thermal degradation temperature. The dynamic mechanical analysis results show that the stiffness of the composite gradually increased with an increase in the weight (%) of PLA in the composites. by increasing their storage modulus values. The peak height of tan δ increased with an increase in the weight (%) of PLA. The 3-point bending test results showed that the bending strength of the starch/cellulose composites increased with the weight (%) of PLA. The SEM images confirmed that PLA showed quite good adhesion with gelatinised starch, which caused the increased stiffness shown by the composites at higher PLA loading. The addition of PLA powder improved water absorption properties of the produced starch/cellulose composites may permit their application in packaging of foods or vegetables.

Acknowledgment This work was supported by the Ministry of Business, Innovation, and Employment (MBIE) of the Government of New Zealand (grant number BPLY1302) through the Biopolymer Network Ltd.

References

Abdel Rahman MA, Tashiro Y, Sonomoto K (2011) Lactic acid production from lignocellulose-derived sugars using lactic acid bacteria: Overview and limits. J Biotechnol 156:296–301.

Ali A, Xie F, Yu L, Liu H, Meng L, Khalid S, Chen L (2018) Preparation and characterization of starch-based composite films reinforced by polysaccharide-based crystals. Composites B 133:122–128.

Avérous L, Fringant C, Moro L (2001) Plasticized starch-cellulose interactions in polysaccharide composites. Polymer 42:6565–6572.

Avérous, L., Moro, L., Dole, P., Fringant, C. (2000). Properties of thermoplastic blends: starch-polycaprolactone. Polymer, 41, 4157–4167.

Carmona VB, De Campos A, Marconcini JM, Mattoso LHC (2014) Kinetics of thermal degradation applied to biocomposites with TPS, PCL and sisal fibres by non-isothermal procedures. J Therm Anal Calorim 115:153–160.

Chen J, Long Z, Wang J, Wu M, Wang F, Wang B, Lv W (2017) Preparation and properties of microcrystalline cellulose/hydroxypropyl starch composite films. Cellulose 24:4449–4459.

518 Corradini E, de Medeiros ES, Carvalho AJF, Curvelo AAS, Mattoso LHC (2006) Mechanical
519 and morphological characterization of starch/zein blends plasticised with glycerol. J
520 Appl Polym Sci 101:4133–4139.
521 Deng Y, Catchmark JM (2014) Insoluble starch composite foams produced through
522 microwave expansion. Carbohydr Polym 111:864–869.
523 Dos Santos BH, De Souza Do Prado K, Jacinto AA, Da Silva Spinacé MA (2018) Influence
524 of sugarcane bagasse fibre size on biodegradable composites of thermoplastic starch. J
525 Renew Mater 6:176–182.
526
527 Edhirej A, Sapuan SM, Jawaid M, Zahari NI (2017) Cassava/sugar palm fibre reinforced
528 cassava starch hybrid composites: Physical, thermal and structural properties. Int J
529 Biologic Macromol 101:75–83.
530 Ghanbari A, Tabarsa T, Ashori A, Shakeri A, Mashkour M (2018) Preparation and
531 characterization of thermoplastic starch and cellulose nanofibers as green
532 nanocomposites: Extrusion processing. Int J Biologic Macromol 112:442–447.
533 Ghorpade VM, Gennadios A, Hanna MA (2001) Laboratory composting of extruded
534 poly(lactic acid) sheets. Bioresour Technol 76:57–61.
535 Glenn GM, Orts WJ, Nobes GAR (2001a) Starch, fibre and $CaCO_3$ effects on the physical
536 properties of foams made by a baking process. Ind Crop Prod 14:201–212.
537 Glenn GM, Orts WJ, Nobes GAR, Gray GM (2001b) In situ laminating process for baked
538 starch-based foams. Ind Crop Prod 14:125–134.
539 Hietala M, Mathew AP, Oksman K (2013) Bionanocomposites of thermoplastic starch and
540 cellulose nanofibers manufactured using twin-screw extrusion. Eur Polym J 49:950–
541 956.

Ibrahim H, Mehanny S, Darwish L, Farag M (2017) A comparative study on the mechanical and biodegradation characteristics of starch-based composites reinforced with different lignocellulosic fibres. J Polym Environ 26:1–14.

Kacurakova M, Smith C, Gidley J, Wilson H (2002) Molecular interaction in bacterial cellulose composite studied by 1D FT-IR and dynamics 2D-FT-IR. Carbohydr Res 337:1145–1153.

Kaushik A, Singh M, Verma G (2010) Green nanocomposites based on thermoplastic starch and steam exploded cellulose nanofibrils from wheat straw. Carbohydr Polym 82:337–345.

Kim J-Y, Huber KC (2016) Preparation and characterization of corn starch-β-carotene composites, Carbohydr Polym 136:394–401.

Lawton JW, Shogren RL, Tiefenbacher KF (1999) Effect of batter solids and starch type on the structure of baked starch foams. Cereal Chem 76:682–687.

Liu D, Dong Y, Bhattacharyya D, Sui G (2017) Novel sandwiched structures in starch/cellulose nanowhiskers (CNWs) composite films. Compos Commun 4:5–9.

Marechal Y, Chanzy H (2000) The hydrogen bond network in I_β cellulose as observed by infrared spectrometry. J Molecular Struc 523:183–186.

Martin O, Schwach E, Avérous L, Couturier Y (2001) Properties of biodegradable multilayer films based on plasticized wheat starch. Stärke 53:372–380.

Masmoudi F, Bessadok A, Dammak M, Jaziri M, Ammar E (2016) Biodegradable packaging materials conception based on starch and polylactic acid (PLA) reinforced with cellulose. Environ Sci Pollut Res Int 23:20904–20914.

Mbey JA, Thomas F (2015) Components interactions controlling starch-kaolinite composite films properties. Carbohydr Polym 117:739–745.

566 Mendes JF, Paschoalin RT, Carmona VB, Sena Neto AR, Marques ACP, Marconcini JM,
567 Mattoso LHC, Medeiros ES, Oliveira JE (2016) Biodegradable polymer blends based
568 on corn starch and thermoplastic chitosan processed by extrusion. Carbohydr Polym
569 137:452–458.
570 Muller J, Jiménez A, González-Martínez C, Chiralt A (2016) Influence of plasticizers on
571 thermal properties and crystallisation behaviour of Poly(lactic acid) films obtained by
572 compression moulding. Polym Int 65:970–978.
573 Muneer F, Andersson M, Koch K, Menzel C, Hedenqvist MS, Gällstedt M, Plivelic TS,
574 Kuktaite R (2015) Nanostructural morphology of plasticized wheat gluten and
575 modified potato starch composites: relationship to mechanical and barrier properties.
576 Biomacromolecules 16:695–705.
577 Noorbakhsh-Soltani SM, Zerafat MM, Sabbaghi S (2018) A comparative study of gelatin and
578 starch-based nano-composite films modified by nano-cellulose and chitosan for food
579 packaging applications. Carbohydr Polym 189:48–55.
580 Orue A, Corcuera MA, Pena C, Eceiza A, Arbelaiz A (2016) Bionanocomposites
581 based on thermoplastic starch and cellulose nanofibers. J Thermoplast Compos Mater
582 29:817–832.
583 Patil NV, Netravali AN (2016) Microfibrillated cellulose-reinforced nonedible starch-based
584 thermoset biocomposites. J Appl Polym Sci 133:43803.
585 Preechawong D, Peesan M, Supaphol P, Rujiravanit R (2005) Preparation and
586 characterisation of starch/poly(L-lactic acid) hybrid foams. Carbohyd Polym 59:329–
587 337.
588 Romero-Bastida CA, Tapia-Blácido DR, Méndez-Montealvo G, Bello-Pérez LA, Velázquez
589 G, Alvarez-Ramirez J (2016) Effect of amylose content and nanoclay incorporation

590 order in physicochemical properties of starch/montmorillonite composites. Carbohydr
591 Polym 152:351–360.
592 Sagnelli D, Kirkensgaard JJK, Giosafatto CVL, Ogrodowicz N, Kruczał K, Mikkelsen MS,
593 Maigret J-E, Lourdin D, Mortensen K, Blennow A (2017) All-natural bio-plastics
594 using starch-beta-glucan composites. Carbohydr Polym 172:237–245.
595 Shirai MA, Grossmann MVE, Mali S, Yamashita F, Garcia PS, Müller CM) (2013)
596 Development of biodegradable flexible films of starch and poly(lactic acid)
597 plasticized with adipate or citrate esters. Carbohydr Polym 92:19–22.
598 Shogren RL, Lawton JW, Doane WM, Tiefenbacher KF (1998) Structure and morphology of
599 baked starch foams. Polymer 39:6649–6655.
600 Spiridon I, Teacă C-A, Bodîrlău R, Bercea M (2013) Behaviour of cellulose reinforced cross-
601 linked starch composite films made with tartaric acid modified starch microparticles. J
602 Polym Environ 21:431–440.
603 Stepto RF (2006) Understanding the processing of thermoplastic starch. Macromol
604 Sympos 245–246:571–577.
605 Subramaniam A (1990) Natural rubber. Ohm RF (Ed), The Vanderbilt Rubber Handbook.
606 R.T. Vanderbilt Company, Norwalk,, USA, pp. 23–43.
607 Swanson CL, Shogren RL, Fanta GF, Imam SH (1993) Starch-plastic materials—Preparation,
608 physical properties, and biodegradability (a review of recent USDA research). J
609 Environ Polym Degrad 1:155–166.
610 Soykeabkaew N, Thanomsilp C, Suwantong O (2015) A review: Starch-based composite
611 foams. Composites A 78:246–263.
612 Soykeabkaew N, Nittaya L, Atitaya N, Natthawut Y, Tawee T (2012) Reinforcing potential
613 of micro- and nano-sized fibers in the starch-based biocomposites. Compos Sci Tech
614 72:845–52.

615 Soykeabkaew N, Supaphol P, Rujiravanit R (2004) Preparation and characterization of jute-
616 and flax-reinforced starch-based composite foams. Carbohyd Polym 58:53–63.
617 Tabassi N, Moghbeli MR, Ghasemi I (2016) Thermoplastic starch/cellulose nanocrystal green
618 composites prepared in an internal mixer. Iranian Polym J 25:45–57.
619 Wang P, Chen F, Zhang H, Meng W, Sun Y, Liu C (2017) Large-scale preparation of jute-
620 fiber-reinforced starch-based composites with high mechanical strength and optimised
621 biodegradability. Stärke 69:1700052.
622 Xu C, Chen C, Wu D (2018) The starch nanocrystal filled biodegradable poly (ε-
623 caprolactone) composite membrane with highly improved properties. Carbohydr
624 Polym 182:115–122.
625 Zhang C-W, Li F-Y, Li J-F, Wang L-M, Xie Q, Xu J, Chen S (2017) A new biodegradable
626 composite with open cell by combining modified starch and plant fibres. Mater
627 Design 120:222–229.
628 Zhou J, Song J, Parker R (2006) Structure and properties of starch-based foams prepared by
629 microwave heating from extruded pellets. Carbohydr Polym 63:466–475.
630
631
632
633
634
635
636
637
638
639

Graphical abstract